



Showcasing research from the Sun lab at the KTH Royal Institute of Technology in Stockholm, Sweden.

Why nature chose the Mn_4CaO_5 cluster as water-splitting catalyst in photosystem II: a new hypothesis for the mechanism of O–O bond formation

A new hypothesis was proposed for the water-oxidation mechanism by the OEC in PSII, involving a charge-rearrangement-induced Mn^{VII} -dioxo species on the dangling Mn^{IV} during the $\text{S}_3 \rightarrow \text{S}_4$ transition. The O–O bond is formed within this Mn^{VII} -dioxo site.

As featured in:



See Biaobiao Zhang and Licheng Sun, *Dalton Trans.*, 2018, 47, 14381.

Cite this: *Dalton Trans.*, 2018, **47**,
14381Received 13th May 2018,
Accepted 6th August 2018

DOI: 10.1039/c8dt01931b

rsc.li/dalton

Why nature chose the Mn_4CaO_5 cluster as water-splitting catalyst in photosystem II: a new hypothesis for the mechanism of O–O bond formation

Biaobiao Zhang ^a and Licheng Sun ^{*a,b}

Resolving the questions, namely, the selection of Mn by nature to build the oxygen-evolving complex (OEC) and the presence of a cubic Mn_3CaO_4 structure in OEC coupled with an additional dangling Mn (Mn4) via μ -O atom are not only important to uncover the secret of water oxidation in nature, but also essential to achieve a blueprint for developing advanced water-oxidation catalysts for artificial photosynthesis. Based on the important experimental results reported so far in the literature and on our own findings, we propose a new hypothesis for the water oxidation mechanism in OEC. In this new hypothesis, we propose for the first time, a complete catalytic cycle involving a charge-rearrangement-induced Mn^{VII} -dioxo species on the dangling Mn4 during the $S_3 \rightarrow S_4$ transition. Moreover, the O–O bond is formed within this Mn^{VII} -dioxo site, which is totally different from that discussed in other existing proposals.

Introduction

The oxygen-evolving complex (OEC) of photosystem II (PSII), which is the most important natural complex for maintaining aerobic life, has existed in photosynthetic organisms on Earth for almost three billion years.^{1,2} Understanding the structure and catalytic mechanism of OEC is motivated not only by humans' desire to discover the secret of natural photosynthesis. It can also provide a blueprint to advance the development of water-oxidation catalysts (WOCs) for artificial photosynthesis for renewable fuel production using solar energy.¹

The general structure of OEC has been determined by a series of X-ray techniques.^{3–7} Fig. 1A shows that the core of OEC comprises a cubic Mn_3CaO_4 structure coupled with an additional dangling Mn (Mn4) via μ -O atom. The entire Mn_4CaO_5 cluster is surrounded by amino acid residues (Y_Z , D1–D61, D1–H190, *etc.*), two Cl^- ions, and many H_2O molecules. However, the pathway of water-oxidation mechanism at the OEC, which proceeds through the Kok cycle via five intermediates (called S_i ($i = 0–4$) states),⁸ remains unknown. Although researchers studying PSII are generally in agreement on the oxidation states⁹ and structures of the meta-

stable S_0 , S_1 , and S_2 intermediates (Fig. 1B),^{3,4,10,11} details of O–O bond formation are still unclear. This is due to lack of experimental evidence for the most important $S_3 \rightarrow S_4$ and $S_4 \rightarrow S_0$ steps, which directly involve the highest oxidized S_4 state that produces oxygen.^{12–14} Currently, two O–O bond formation pathways are widely discussed: water nucleophilic attack mechanism^{14,15} and oxo-oxyl radical coupling mechanism,^{16–18} which involve a Mn^{V} -oxo electrophile and a Mn^{IV} -oxyl radical as the active S_4 intermediate (Fig. 1B), respectively. However, the existence of a Mn^{V} -oxo electrophile or Mn^{IV} -oxyl radical in OEC catalysis has not been experimentally proved. Hence, mechanism of water oxidation by the Mn_4CaO_5 cluster is still an open question, requiring scientists to propose more appropriate answers.

The current proposed mechanism for water oxidation by the Mn_4CaO_5 cluster is far from complete and cannot effectively explain the selection of Mn by nature, the construction of OEC from multiple Mn ions, and the presence of a dangling Mn4 outside the cubic structure. Herein, we propose a Mn^{VII} -dioxo-based mechanism for O–O bond formation by the Mn_4CaO_5 cluster. This mechanism is distinct from the widely discussed water nucleophilic attack and oxo-oxyl radical coupling mechanisms. Our mechanism suggests that after charge accumulation in the first three steps, charge rearrangement occurs in the fourth step to form a Mn^{VII} -dioxo site on the dangling Mn4, where the O–O bond forms in the S_4 state. This Mn^{VII} -dioxo-based mechanism may open new possibilities for revealing the actual mechanism of water oxidation in PSII, and

^aDepartment of Chemistry, KTH Royal Institute of Technology, 10044 Stockholm, Sweden. E-mail: lichengs@kth.se

^bState Key Laboratory of Fine Chemicals, Institute of Artificial Photosynthesis, DUT-KTH Joint Education and Research Center on Molecular Devices, Dalian University of Technology (DUT), 116024 Dalian, China



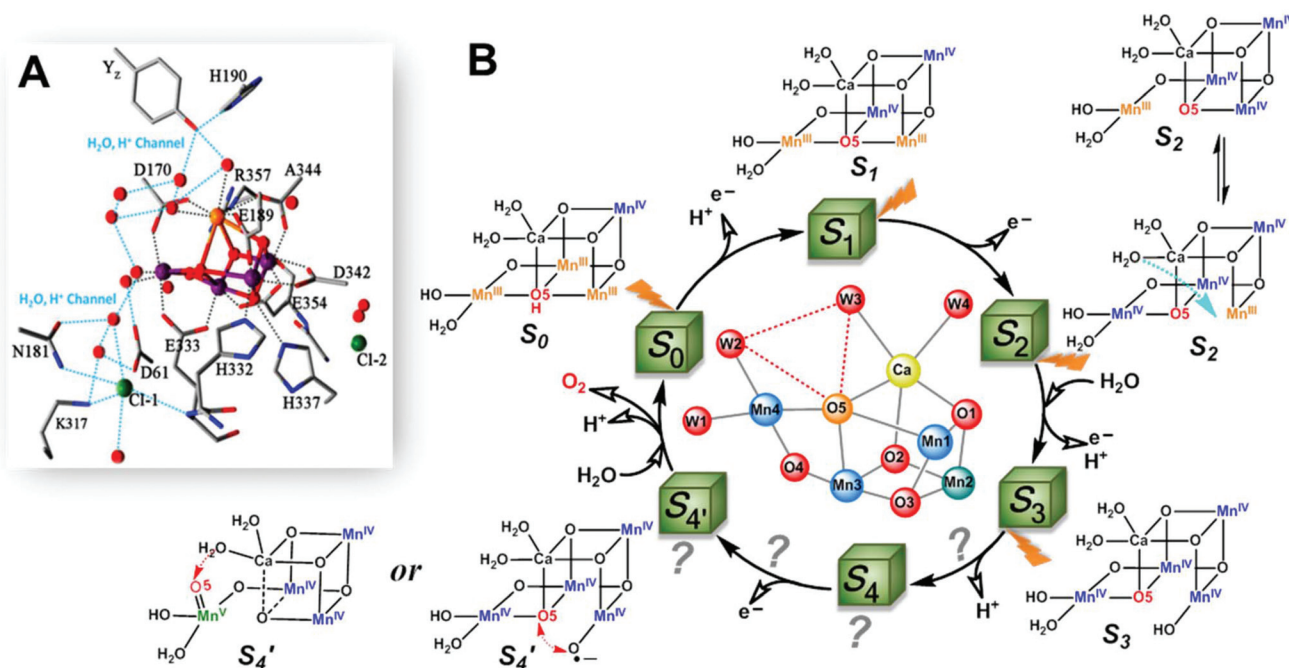


Fig. 1 (A) Structure of Mn_4CaO_5 cluster of the OEC in PSII.³ (B) Extended classic Kok cycle^{8,19} for water oxidation in PSII, involving electron transfer and proton release, and the widely proposed structures of intermediate “S” states. S_i ($i = 0-4$) states represent oxidation states of the Mn_4CaO_5 cluster relative to the S_0 state. S_1 is the only dark-stable state. S_2 state exists as two interconverting isomers: “open” and “closed” configurations.¹⁰ A significant structural change occurs in the S_3 state.¹⁹⁻²³ S_4 and S_4' states are hypothetical states without experimental evidence, due to their ultra-short life-times^{14,19} and related reaction steps being unclear.

consequently offer cogent guidance for developing more efficient synthetic WOCs for artificial photosynthesis.

Proposing the Mn^{VII} species involved mechanism

Aside from the abundance of Mn on Earth, a fundamental reason for nature to incorporate Mn in OEC could be the specificity of its redox chemistry.^{24,25} It is reasonable to consider mechanism of water oxidation by the Mn_4CaO_5 cluster in terms of the particular redox chemistry of Mn. For first-row transition metals in the periodic table, from Sc to Zn, the highest accessible valency and number of accessible valencies first increase up to Mn and then decrease toward Zn, which only has a valency of +2.²⁴ Therefore, Mn has the highest oxidation state (Mn^{VII}), and the largest number of oxidation states, *i.e.*, Mn is the only metal (at least among those involved in plants) that can carry five charges (from Mn^{II} to Mn^{VII}). Furthermore, Mn participates in many disproportionation reactions between two or multiple Mn ions. The unique redox chemistry of Mn makes it an ideal element for building the OEC, in which accumulation of four charges is needed to oxidize two water molecules to molecular oxygen. Based on these unique features of Mn and experimental evidences presented below, we propose a new mechanism for water oxidation by the Mn_4CaO_5 cluster in PSII, which involves charge-rearrangement-induced Mn^{VII} -dioxo species.

In this new mechanism, we propose that first three steps, *i.e.*, $S_0 \rightarrow S_1$, $S_1 \rightarrow S_2$, and $S_2 \rightarrow S_3$, are the charge accumulation steps. As shown in Fig. 2, electron transfers, proton transfers,

and structural changes during these three steps are consistent with the widely accepted processes with abundant experimental evidences.^{9,12-14} The dark-stable S_1 [III, IV, IV, III] state, which evolves from the S_0 [III, IV, III, III] state *via* a proton-coupled electron-transfer process, is transformed into the S_2 state after loss of one electron (please note that the order of oxidation states follows the numbering of Mn atoms in Fig. 2). In the following crucial $S_2 \rightarrow S_3$ step, W3 H_2O on the Ca site inserts into the open position between Ca and O5^{17,20,26} and forms a new O5 for the next catalytic cycle. The original O5 is pulled towards Mn4 as a π -donating ligand. Loss of one proton and another electron gives the S_3 intermediate with oxidation states [IV, IV, IV, IV]. We believe that charge accumulation on the Mn_4CaO_5 cluster is the driving force for insertion of the W3 H_2O , because one negatively charged ligand is needed to stabilize the S_3 [IV, IV, IV, IV] state. The insertion of W3 H_2O and subsequent deprotonation help to balance the positive charges accumulated on the Mn core structure after the first three steps of oxidation.

After accumulation of three charges on the Mn_4CaO_5 cluster at the S_3 state, the oxidation state of Mn ions in the Mn_4CaO_5 cluster is [IV, IV, IV, and IV]. According to the Latimer diagram of Mn, this is the highest state that can be reached through a one-electron oxidation (Scheme 1). Thus, in contrast to the first three oxidation steps, during the $S_3 \rightarrow S_4$ step, the fourth charge obtained from P680⁺ is retained for a longer period on Y_z' than that in the first three steps. This results in the observation of a $S_3\text{-Y}_z'$ state^{19,21} because the





Fig. 2 Proposed catalytic mechanism for water oxidation by Mn_4CaO_5 cluster in PSII involving Mn^{VII} -dioxo species. Charge disproportionation of Mn_4CaO_5 cluster at the $\text{S}_3\text{-Y}_Z'$ state after accumulation of three charges, *i.e.*, charge rearrangement, leads to the formation of a super-active S'_4 [III, III, IV, VII] state after the $\text{S}_3 \rightarrow \text{S}_4$ step. An O–O bond forms within the Mn^{VII} -dioxo site (between W2 and O5) during the $\text{S}_4 \rightarrow \text{S}'_4$ step. W2, O5, and W3 all participate in O_2 evolution.



Scheme 1 The Latimer diagram for Mn illustrates its standard reduction potentials (in 1 M acid) at oxidation states from +7 to 0.

direct oxidation of [IV, IV, IV, IV] to [V, IV, IV, IV] by Y_Z' may not be the lowest energy pathway. To accept the fourth charge from Y_Z' , *i.e.*, to further oxidize the Mn_4CaO_5 cluster, a charge rearrangement (*i.e.* disproportionation) occurs within the four Mn^{IV} ions in the S_3 state. This is accompanied with release of a proton, resulting in an S_4 [III, III, III, VII] resting state with a Mn^{VII} -dioxo site. The fourth oxidation by the P680^+ can be a driving force that triggers the acceleration of charge rearrangement because it introduces the Y_Z' , which changes the positively charged environment around the Mn_4CaO_5 cluster and the pK_a balance of proton transfer channels.^{20,27,28}

These multiple processes involved in the $\text{S}_3 \rightarrow \text{S}_4$ step, including storage of one charge on Y_Z' , release of one proton, charge rearrangement, and formation of the Mn^{VII} -dioxo site, are crucial for restoring the severely charged Mn cluster and producing a standby state to accept a fourth charge and form the O–O bond. Indeed, significant structural rearrangements

have been experimentally observed during the $\text{S}_3\text{-Y}_Z' \rightarrow \text{S}_4 \rightarrow \text{S}_0$ steps.^{19,21} After such charge rearrangement, the S_4 transition state [III, III, III, VII] is easily oxidized by its paired Y_Z' to the active S'_4 [III, III, IV, VII] state. This highly active S'_4 species immediately releases a molecular oxygen *via* a peroxo transition state S''_4 [III, III, IV, V] and is transformed back to the S_0 [III, IV, III, III] state by binding one ready H_2O , supplied from the ASP61/ Cl^- water channel, to vacant sites on the dangling Mn4 and losing one proton, thus completing one catalytic cycle.

In this new mechanism, two unique and attractive points are to be necessarily discussed in detail: (1) charge rearrangement involving disproportionation of 4 Mn^{IV} into 3 Mn^{III} and 1 Mn^{VII} (*i.e.*, $\text{Mn}^{\text{IV}}\text{-Mn}^{\text{IV}}\text{-Mn}^{\text{IV}}\text{-Mn}^{\text{IV}} \rightarrow \text{Mn}^{\text{VII}}\text{-Mn}^{\text{III}}\text{-Mn}^{\text{III}}\text{-Mn}^{\text{III}}$), and (2) O–O bond formation at the Mn^{VII} -dioxo site. Although we did not perform special verifiable experimental studies for this article, there are sufficient published experimental results to support these two essential proposals.

Disproportionation of $\text{Mn}^{\text{IV}}\text{-Mn}^{\text{IV}}\text{-Mn}^{\text{IV}}\text{-Mn}^{\text{IV}}$ to $\text{Mn}^{\text{VII}}\text{-Mn}^{\text{III}}\text{-Mn}^{\text{III}}\text{-Mn}^{\text{III}}$

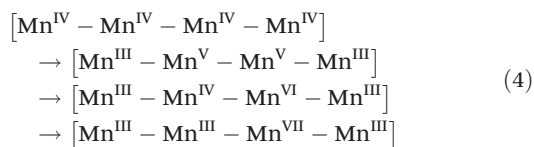
The mechanism of water oxidation by Mn^{IV} sulphate was investigated by Shilov *et al.* ca. 40 years ago.²⁹ Their experimental



results showed that the intermediate involved in oxygen evolution is a Mn^{VII} species generated by disproportionation of Mn^{IV} ions.^{29,30} The detailed kinetic study of this reaction indicated that charge disproportionation of 4 Mn^{IV} to 1 Mn^{VII} and 3 Mn^{III} regularly happens under Mn^{IV}-rich conditions. Furthermore, a kinetic study by Dzhabiev *et al.* showed that a tetranuclear Mn^{IV} intermediate may be involved in the charge disproportionation of 4 Mn^{IV} to 1 Mn^{VII} and 3 Mn^{III} (eqn (1)).³¹



Moreover, formation of MnO₄⁻ species has been observed during water oxidation using several Mn based catalytic systems.^{32–36} For example, Kaneko *et al.* reported that MnO₄⁻ was formed from the oxidation of [(bpy)₂Mn(μ-O)₂Mn(bpy)₂] (Mn-bpy, bpy = 2,2'-bipyridine).³³ As shown in eqn (2), they suggested that two molecules of Mn-bpy dimer, *i.e.*, four Mn cores, are involved in MnO₄⁻ formation.



Similarly, Brudvig *et al.* observed the formation of MnO₄⁻ while studying water oxidation by [(H₂O)(tpy)Mn(μ-O)₂Mn(tpy)(H₂O)] (Mn-tpy, tpy = 2,2':6',2''-terpyridine) dimer catalysts.^{32,34} They proposed that MnO₄⁻ formed *via* disproportionation of [(tpy)(O)Mn^V(μ-O)₂Mn^V(tpy)(H₂O)] (eqn (3)). Furthermore, Yagi *et al.* found that two molecules of Mn-tpy dimer were involved in the rate-determining step of MnO₄⁻ formation by kinetic analysis. This is consistent with proposal by Kaneko *et al.* These experimental observations strongly support that one possible evolution pathway for a [IV, IV, IV, IV] state is to disproportionate into a [VII, III, III, III] state. A detailed process of charge rearrangement is proposed as shown in eqn (4), in which the transformation from Mn^{IV}-Mn^{VI} to Mn^{VII}-Mn^{III} is a fast step.³⁰

Although theoretical studies are not sufficient to explain this complicated process, a Latimer diagram of Mn can preliminarily help us understand why multiple Mn ions are involved in the generation of Mn^{VII} species instead of a step by step one-electron oxidation (Scheme 1). The Latimer diagram of Mn shows that oxidation potential from Mn^{IV} to Mn^V is 4.27 V, which is much higher than all other redox potentials of Mn. This implies that the stepwise one-electron oxidation of Mn^{IV} to Mn^{VII} may need very high energy. This also explains why Mn^V is the only species missing in the Pourbaix diagram of Mn and why MnO₄⁻ lies in close proximity to MnO₂.

However, the oxidation potentials of PSII are sufficient to generate a high-valent Mn^{VII} site in the Mn₄CaO₅ cluster. In the Pourbaix diagram for Mn, theoretical potential for the formation of MnO₄⁻ at pH 7 is 1.05 V.³⁶ The estimated redox

potentials for P680/P680⁺ and Y_Z/Y_Z[•] are approximately +1.26 and +1.21 V, respectively,³⁷ and are thermodynamically adequate for initiating the formation of Mn^{VII} species. Indeed, Mn^{II} can be oxidized to Mn^{VII} by moderate one-electron oxidants²⁹ such as Ru(bipyridine)₃³⁺ with an oxidation potential of +1.26 V, which is close to the potentials of P680⁺ and Y_Z[•].

These analyses together with the consideration of the facts of PSII, *i.e.*, the unique dangling Mn4 site and existence of the S₃-Y_Z[•] state, reasonably support the disproportionation of the [IV, IV, IV, IV] state to a [III, III, III, VII] state during the S₃ → S₄ transition.

O–O bond formation within the Mn^{VII}-dioxo site

Oxygen evolution at Mn^{VII}-dioxo site is thermodynamically possible, but kinetically hampered. For example, it is well known that MnO₄⁻ can evolve O₂, but the rate is very slow.³⁸

However, the rate of oxygen evolution from Mn^{VII}-dioxo site can be greatly enhanced by various promoters. For example, MnO₂ has been known as a catalyst for oxygen evolution from MnO₄⁻ by Skrabal since 1910.³⁸ Shafirovich *et al.* studied the mechanism of oxygen formation during oxidation of water by Mn^{IV} sulfate. They suggested a mechanism (Fig. 3A) where a Mn^{IV}-Mn^{VII} surface complex is the active intermediate for O–O bond formation.^{29–31} Interestingly, a crystalline Mn^{IV}-Mn^{VII} complex, (H₃O)₂-[Mn^{IV}(Mn^{VII}O₄)₆]·11H₂O, immediately evolves oxygen when kept at or over -4 °C (Fig. 3B).³⁹ When MnO₄⁻ is activated by a strong Lewis acid such as BF₃, O₂ is rapidly evolved *via* intramolecular coupling of Mn^{VII}-dioxo site (Fig. 3C).⁴⁰ During photo-induced oxygen evolution from MnO₄⁻, Lee *et al.* investigated the presence of an excited state of MnO₄⁻, which is a much more active oxidant than permanganate itself and the subsequent formation of a Mn^V-dioxo intermediate prior to oxygen evolution (Fig. 3D).⁴¹ A Mn^{VII}=O species has also been proposed as an essential intermediate for a Mn^V-nitrido complex during Ce^{IV}-driven water oxidation (Fig. 3E).⁴² In 2017, a highly reactive pendant Mn^{VII}=O moiety on a cubic Mn-nitride complex has been reported as a synthetic structural model of the proposed S₄ state in PSII (Fig. 3F).⁴³

Very recently, we reported the presence of an essential Mn^{VII}-dioxo intermediate in a synthetic *c*-disordered δ-MnO_x-based water oxidation catalyst (*i.e.*, MnO_x-300),⁴⁵ where a Mn^{IV}-O-Mn^{VII}=O was proposed as the active species for O–O bond formation.⁴⁴ As shown in Fig. 4, one active Mn site and three related Mn atoms of the manganese oxides are suggested to participate actively in the catalysis. After multiple electrochemical oxidations of the active site, the initial [Mn^{III}Mn^{III}Mn^{IV}(HO-Mn^{III}-OH₂)] state is oxidized to [Mn^{IV}Mn^{IV}Mn^{IV}(HO-Mn^{IV}=O)] accompanied by the loss of three electrons and two protons. [Mn^{IV}Mn^{IV}Mn^{IV}(HO-Mn^{IV}=O)] is assumed to undergo charge rearrangement with release of one proton, resulting in a resting [Mn^{III}Mn^{III}Mn^{III}Mn^{VII}(=O)₂] state. A structural moiety of this intermediate has been proved by a characteristic CV reduction peak at 0.93 V and an IR absorption frequency of 912 cm⁻¹, which strictly corresponds to the occurrence of water-oxidation





Fig. 3 Highly reactive Mn^{VII} species and related O₂ evolution reactions. (A) Pathway for oxygen evolution from MnO₄⁻, catalysed by Mn^{IV} ion.²⁹ (B) Structure of [Mn^{IV}(Mn^{VII}O₄)₆]²⁻ complex.³⁹ (C) Mechanism for fast oxygen evolution from MnO₄⁻, activated by BF₃, a strong Lewis acid.⁴⁰ (D) Proposed structures of intermediates for O₂ evolution from photodecomposition of MnO₄⁻.⁴¹ (E) Mechanism for water oxidation by Mn^V-nitrido molecular catalyst.⁴² (F) Structure of cubic Mn-nitride complex with pendant Mn^{VII}=O moiety.⁴³

reaction. Moreover, several experimental evidences demonstrated that this surface-bonded Mn^{VII}-dioxo intermediate is more prone to oxidation than the free MnO₄⁻. However, we consider it as a resting state instead of a final active species for O–O bond formation since this Mn^{VII}-dioxo intermediate has a long life time. Subsequently, the Mn^{III} ion directly bonded to the dangling Mn^{VII}=O site is thought to be further oxidized to Mn^{IV}, which drastically increases reactivity of the Mn^{VII}=O site, forming the active state [Mn^{III}Mn^{III}Mn^{IV}Mn^{VII}(=O)₂] state for oxygen evolution. Results of this study can be experimental evidences to support the assumption that an activated permanganate-like Mn^{VII}=O moiety is highly reactive and it may be present during the catalytic cycle of water oxidation in PSII.

The above examples clearly show that O–O bond formation from species with activated permanganate-like Mn^{VII}=O moiety is a fast and efficient pathway for oxygen evolution. In contrast, a fast O–O bond formation mechanism from Mn^{IV}=O or Mn^V=O species is not commonly available in the published studies on oxygen evolution reaction. Since the turnover frequency of PSII is about 100–400 s⁻¹,³⁶ it is necessary to consider a fast pathway for the O–O bond formation, involved in the mechanism of water oxidation by PSII.

Lastly, we emphasize that in this new proposed mechanism, the essential charge rearrangement involved in the steps of S₃-Y_Z[•] → S₄ → S₀ is consistent with the kinetic studies where a slow kinetic phase involving a structural rearrangement has



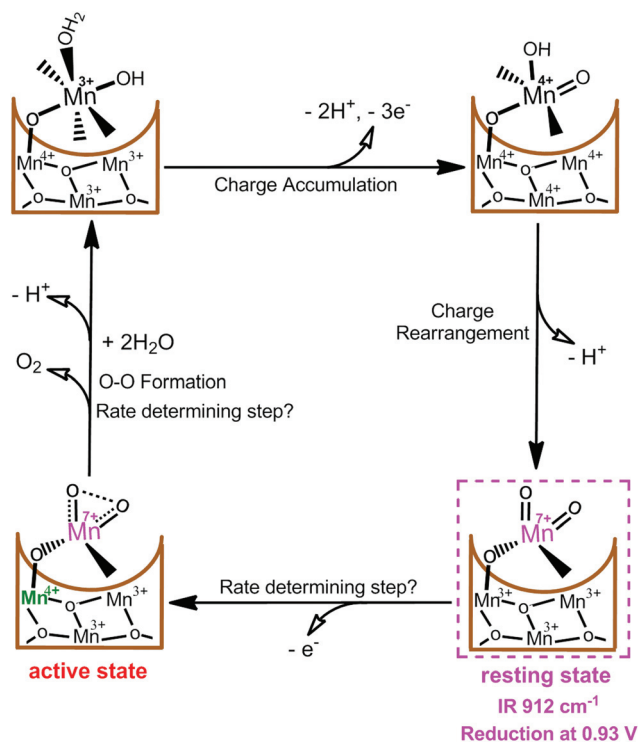


Fig. 4 Proposed catalytic cycle in MnO_x -300-catalyzed water-oxidation reaction.⁴⁴

been strongly suggested,^{19,21–23,27,28} giving a possible explanation to this slow kinetic phase. Two molecules of water are transferred into the Mn_4CaO_5 cluster during each catalytic cycle: one from the Ca water channel (as the successor of O5 for the next catalytic cycle) and one from the Asp61 water channel (for the new W2) consumed for forming O_2 . This is consistent with the fact that the proton/water channels in PSII are closely related to the Ca site and the Mn4 site.⁴⁶ This finding also agrees with the fact that W2, W3 and O5 are usually considered as the O substrates involved in O–O bond formation.⁴⁶

Based on our findings, we prefer this mechanism that involves $\text{Mn}^{\text{VII}}=\text{O}$ moiety and O–O bond formation compared to the coupling of O5 and O of W2 for water oxidation by the OEC. However, without experimental evidence from direct studies on the OEC, particularly for the $\text{S}_3 \rightarrow \text{S}_4$ step, other potential O–O bond formation pathways may be possible, for example, O–O bond formation from O5 and the new O (O6) on Mn1^{17,18,47} or from O4 and O of W1.⁴⁸

Conclusions

Involvement of Mn^{VII} in the O–O bond formation step is a highly appropriate alternative mechanism for water-oxidation catalysis by the Mn_4CaO_5 cluster. This mechanism involves a complete catalytic cycle with reasonable valency changes, structural transformations, and O–O bond formation steps. In this new mechanism, we propose that Mn4 is the active site for the O–O bond formation in the S_4 state by forming an essential

Mn^{VII} -dioxo species. This Mn4 site also functions as a gate for releasing protons from the Mn_4CaO_5 cluster. Mn1, Mn2, and Mn3 sites, within the cubane, function as a battery for charge storage in the first three steps. During the $\text{S}_3 \rightarrow \text{S}_4$ step, all stored charges accumulate on Mn4 to form the appropriate Mn^{VII} -dioxo state, which subsequently triggers O–O bond formation and oxygen evolution. Hence, OEC is constructed as a Mn_3CaO_4 cubane coupled with a dangling Mn4. In addition, OEC has an extremely open coordination sphere that is located in the water and proton channels and approaches the redox mediator Y_Z .

Therefore, we suggest that synthetic multinuclear Mn complexes could be promising candidates for efficient artificial WOCs. Different coordination environments should be considered in the ligand structure design for different types of Mn cores with specific roles, *i.e.*, multiple Mn cores for charge storage and Mn with open coordination sites for handling substrate water, proton release, and O–O bond formation. Furthermore, special attention should be paid to the ligands that are needed to stabilize the Mn^{VII} site.

Finally, on the basis of our new mechanistic proposal, we can answer the question in the title: why did nature choose the Mn_4CaO_5 cluster as the catalyst for water oxidation in PSII?

- Mn is abundant in the Earth, has rich redox chemistry, and can bear four charges by varying its valencies between Mn^{III} and Mn^{VII} .

- Four Mn can coordinate and create the Mn^{VII} -dioxo site *via* charge disproportionation of four Mn^{IV} , which is unique, *i.e.*, distinguishable from other 3 Mn ions by being placed outside the cubane structure.

- Five μ -oxo bridges are essential, with one (O5) available for O–O bond formation and the other four for balancing the positive charges. These bridges can also prevent the integral Mn_4CaO_5 cluster structure from falling apart (maintaining cooperation among four Mn and one Ca).

- Ca is needed as a “taxi stand” for the essential substrate water molecules before they are transferred to the open site during the $\text{S}_2 \rightarrow \text{S}_3$ step to regenerate a new O5 for the next catalytic cycle.

Therefore, as an economic and perfect “team-playing” catalyst, the Mn_4CaO_5 cluster was chosen by nature for water oxidation in PSII three billion years ago. Since investigations and conclusions on the mechanism of oxygen evolution in PSII are still far from clear, we hope our new hypothesis opens new possibilities for uncovering the secrets of water oxidation in PSII.

Conflicts of interest

The authors declare no competing interests.

Acknowledgements

We acknowledge financial support of this work by the Swedish Research Council (2017-00935), Swedish Energy Agency, Knut



and Alice Wallenberg Foundation, and the National Basic Research Program of China (973 program, 2014CB239402). We thank Professor Christina Moberg at KTH for reviewing the manuscript and the valuable discussions.

References

- J. P. McEvoy and G. W. Brudvig, *Chem. Rev.*, 2006, **106**, 4455–4483.
- S. A. Crowe, L. N. Dossing, N. J. Beukes, M. Bau, S. J. Kruger, R. Frei and D. E. Canfield, *Nature*, 2013, **501**, 535–538.
- M. Suga, F. Akita, K. Hirata, G. Ueno, H. Murakami, Y. Nakajima, T. Shimizu, K. Yamashita, M. Yamamoto, H. Ago and J. R. Shen, *Nature*, 2015, **517**, 99–103.
- Y. Umena, K. Kawakami, J. R. Shen and N. Kamiya, *Nature*, 2011, **473**, 55–60.
- K. N. Ferreira, T. M. Iverson, K. Maghlaoui, J. Barber and S. Iwata, *Science*, 2004, **303**, 1831–1838.
- A. Zouni, H.-T. Witt, J. Kern, P. Fromme, N. Krauß, W. Saenger and P. Orth, *Nature*, 2001, **409**, 739–743.
- B. Loll, J. Kern, W. Saenger, A. Zouni and J. Biesiadka, *Nature*, 2005, **438**, 1040–1044.
- B. Kok, B. Forbush and M. McGloin, *Photochem. Photobiol.*, 1970, **11**, 457–475.
- V. Krewald, M. Retegan, N. Cox, J. Messinger, W. Lubitz, S. DeBeer, F. Neese and D. A. Pantazis, *Chem. Sci.*, 2015, **6**, 1676–1695.
- D. A. Pantazis, W. Ames, N. Cox, W. Lubitz and F. Neese, *Angew. Chem., Int. Ed.*, 2012, **51**, 9935–9940.
- T. Lohmiller, V. Krewald, A. Sedoud, A. W. Rutherford, F. Neese, W. Lubitz, D. A. Pantazis and N. Cox, *J. Am. Chem. Soc.*, 2017, **139**, 14412–14424.
- J. Yano and V. Yachandra, *Chem. Rev.*, 2014, **114**, 4175–4205.
- M. Perez-Navarro, F. Neese, W. Lubitz, D. A. Pantazis and N. Cox, *Curr. Opin. Chem. Biol.*, 2016, **31**, 113–119.
- D. J. Vinyard, S. Khan and G. W. Brudvig, *Faraday Discuss.*, 2015, **185**, 37–50.
- J. Barber, *Nat. Plants*, 2017, **3**, 17041.
- P. E. M. Siegbahn, *Acc. Chem. Res.*, 2009, **42**, 1871–1880.
- M. Suga, F. Akita, M. Sugahara, M. Kubo, Y. Nakajima, T. Nakane, K. Yamashita, Y. Umena, M. Nakabayashi, T. Yamane, T. Nakano, M. Suzuki, T. Masuda, S. Inoue, T. Kimura, T. Nomura, S. Yonekura, L.-J. Yu, T. Sakamoto, T. Motomura, J.-H. Chen, Y. Kato, T. Noguchi, K. Tono, Y. Joti, T. Kameshima, T. Hatsui, E. Nango, R. Tanaka, H. Naitow, Y. Matsuura, A. Yamashita, M. Yamamoto, O. Nureki, M. Yabashi, T. Ishikawa, S. Iwata and J.-R. Shen, *Nature*, 2017, **543**, 131–135.
- P. E. M. Siegbahn, *Proc. Natl. Acad. Sci. U. S. A.*, 2017, **114**, 4966–4968.
- M. Haumann, P. Liebisch, C. Müller, M. Barra, M. Grabolle and H. Dau, *Science*, 2005, **310**, 1019–1021.
- H. Sakamoto, T. Shimizu, R. Nagao and T. Noguchi, *J. Am. Chem. Soc.*, 2017, **139**, 2022–2029.
- H. Bao and R. L. Burnap, *Proc. Natl. Acad. Sci. U. S. A.*, 2015, **112**, E6139–E6147.
- I. Zaharieva, H. Dau and M. Haumann, *Biochemistry*, 2016, **55**, 6996–7004.
- M. Haumann, C. Müller, P. Liebisch, L. Iuzzolino, J. Dittmer, M. Grabolle, T. Neisius, W. Meyer-Klaucke and H. Dau, *Biochemistry*, 2005, **44**, 1894–1908.
- F. A. Armstrong, *Philos. Trans. R. Soc., B*, 2008, **363**, 1263–1270.
- R. J. Pace, R. Stranger and S. Petrie, *Dalton Trans.*, 2012, **41**, 7179–7189.
- M. Capone, D. Narzi, D. Bovi and L. Guidoni, *J. Phys. Chem. Lett.*, 2016, **7**, 592–596.
- M. R. Razeghifard and R. J. Pace, *Biochemistry*, 1999, **38**, 1252–1257.
- G. Renger, *Biochim. Biophys. Acta*, 2001, **1503**, 210–228.
- V. Y. Shafirovich, N. K. Khannanov and A. E. Shilov, *J. Inorg. Biochem.*, 1981, **15**, 113–129.
- V. Y. Shafirovich, *Kinet. Katal.*, 1978, **19**, 1502–1507.
- T. S. Dzhabiev, *Kinet. Katal.*, 1989, **30**, 1219–1224.
- J. Limburg, J. S. Vrettos, L. M. Liable-Sands, A. L. Rheingold, R. H. Crabtree and G. W. Brudvig, *Science*, 1999, **283**, 1524–1527.
- R. Ramaraj, A. Kira and M. Kaneko, *Chem. Lett.*, 1987, **16**, 261–264.
- J. Limburg, G. W. Brudvig and R. H. Crabtree, *J. Am. Chem. Soc.*, 1997, **119**, 2761–2762.
- M. Yagi and K. Narita, *J. Am. Chem. Soc.*, 2004, **126**, 8084–8085.
- M. M. Najafpour, G. Renger, M. Holynska, A. N. Moghaddam, E. M. Aro, R. Carpentier, H. Nishihara, J. J. Eaton-Rye, J. R. Shen and S. I. Allakhverdiev, *Chem. Rev.*, 2016, **116**, 2886–2936.
- M. Grabolle and H. Dau, *Biochim. Biophys. Acta*, 2005, **1708**, 209–218.
- A. Skrabal, *Anorg. Allg. Chem.*, 1910, **68**, 48–51.
- B. Krebs and K.-D. Hasse, *Angew. Chem., Int. Ed. Engl.*, 1974, **13**, 603.
- S. M. Yiu, W. L. Man, X. Wang, W. W. Lam, S. M. Ng, H. K. Kwong, K. C. Lau and T. C. Lau, *Chem. Commun.*, 2011, **47**, 4159–4161.
- D. G. Lee, C. R. Moylan, T. Hayashi and J. I. Braurnan, *J. Am. Chem. Soc.*, 1987, **109**, 3003–3010.
- L. Ma, Q. Wang, W. L. Man, H. K. Kwong, C. C. Ko and T. C. Lau, *Angew. Chem., Int. Ed.*, 2015, **54**, 5246–5249.
- S. Vaddypally, S. K. Kondaveeti, S. Karki, M. M. Van Vliet, R. J. Levis and M. J. Zdilla, *J. Am. Chem. Soc.*, 2017, **139**, 4675–4681.
- B. Zhang, Q. Daniel, L. Fan, T. Liu, Q. Meng and L. Sun, *iScience*, 2018, **4**, 144–152.
- B. Zhang, H. Chen, Q. Daniel, B. Philippe, F. Yu, M. Valvo, Y. Li, R. B. Ambre, P. Zhang, F. Li, H. Rensmo and L. Sun, *ACS Catal.*, 2017, **7**, 6311–6322.
- J. R. Shen, *Annu. Rev. Plant Biol.*, 2015, **66**, 23–48.
- H. Isobe, M. Shoji, J. R. Shen and K. Yamaguchi, *Inorg. Chem.*, 2016, **55**, 502–511.
- K. Kawashima, T. Takaoka, H. Kimura, K. Saito and H. Ishikita, *Nat. Commun.*, 2018, **9**, 1247.

